HITS-CLIP analysis of human ALKBH8 reveals interactions with fully processed substrate tRNAs and with specific noncoding RNAs

IVANA CAVALLIN,[1] MAREK BARTOSOVIC,[1,5] TOMAS SKALICKY,[1,2] PRAVEENKUMAR RENGARAJ,[1] MARTIN DEMKO,[1] MARTINA CHRISTINA SCHMIDT-DENGLER,[3] ALEKSEJ DRINO,[4] MARK HELM,[3] and STEPANKA VANACOVA[1]

[1]Central European Institute of Technology, Masaryk University, 625 00 Brno, Czech Republic
[2]Institute of Parasitology, Biology Centre, Czech Academy of Sciences, 370 05 České Budějovice, Czech Republic
[3]Johannes Gutenberg-Universität Mainz, Institute of Pharmaceutical and Biomedical Science (IPBS), D-55128 Mainz, Germany
[4]Medical University of Vienna, Center for Anatomy and Cell Biology, 1090 Vienna, Austria

ABSTRACT

Transfer RNAs acquire a large plethora of chemical modifications. Among those, modifications of the anticodon loop play important roles in translational fidelity and tRNA stability. Four human wobble U–containing tRNAs obtain 5-methoxycarbonylmethyluridine (mcm^5U_{34}) or 5-methoxycarbonylmethyl-2-thiouridine ($mcm^5s^2U_{34}$), which play a role in decoding. This mark involves a cascade of enzymatic activities. The last step is mediated by alkylation repair homolog 8 (ALKBH8). In this study, we performed a transcriptome-wide analysis of the repertoire of ALKBH8 RNA targets. Using a combination of HITS-CLIP and RIP-seq analyses, we uncover ALKBH8-bound RNAs. We show that ALKBH8 targets fully processed and CCA modified tRNAs. Our analyses uncovered the previously known set of wobble U–containing tRNAs. In addition, both our approaches revealed ALKBH8 binding to several other types of noncoding RNAs, in particular C/D box snoRNAs.

Keywords: ALKBH8; Trm9; wobble uridine modification; mcm^5U; mcm^5s^2U; HITS-CLIP

INTRODUCTION

Chemical RNA modifications have emerged as an important regulator of gene expression in many living systems. In tRNAs, modifications of the anticodon residues allow the decoding capacity to expand. Wobbling is the pairing of the third codon nucleotide with the first anticodon nucleotide, termed the wobble nucleotide, by a non-Watson–Crick bond. This allows recognition of noncognate codons (Crick 1966), and consequently enables substitution of a missing tRNA decoder or regulates translation (Grosjean et al. 2010; Endres et al. 2015b). In bacteria and organelles, there are cases of superwobbling where an unmodified wobble uridine can decode all four nucleotides (Inagaki et al. 1995; Rogalski et al. 2008; Alkatib et al. 2012). However, in the eukaryotic cytosol, wobble uridine is almost invariably modified (Yokoyama et al. 1985; Schaffrath and Leidel 2017). Modified wobble uridine is most commonly found in split codon boxes, and it is presumed that it prevents mistranslation of the pyrimidine encoded amino acid (Johansson et al. 2008).

To date, decoding by wobble uridine has been studied mainly in yeast. Analysis of purified tRNAs identified different modifications of wobble uridines (Fig. 1A; Supplemental Fig. S1A; Smith et al. 1973; Kobayashi et al. 1974; Kuntzel et al. 1975; Randerath et al. 1979; Yamamoto et al. 1985; Keith et al. 1990; Glasser et al. 1992; Szweykowska-Kulinska et al. 1994; Lu et al. 2005; Johansson et al. 2008). These modifications are formed in several steps. The first step in the wobble uridine modification is catalyzed by the Elongator complex. The Elongator is composed of six subunits Elp1–Elp6 (Huang 2005; Dauden et al. 2017). The Elp3 subunit catalyzes the transfer of the carboxymethyl (cm) residue to the 5-position of uridine (Selvadurai et al. 2014). Trm9 performs methylation of 5-carboxymethyluridine (cm^5U) and 5-carboxymethyl-2-thiouridine (cm^5s^2U) to

[5]**Present address:** Division of Molecular Neurobiology, Solnavägen 9171 65 Solna, Sweden
Corresponding author: stepanka.vanacova@ceitec.muni.cz
Article is online at http://www.rnajournal.org/cgi/doi/10.1261/rna.079421.122.

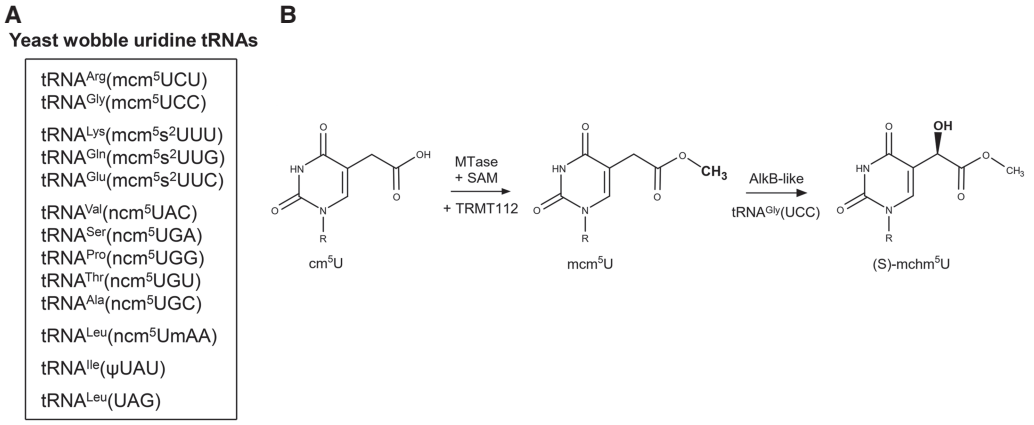

FIGURE 1. Wobble uridine tRNA modifications and ALKBH8 activities. (*A*) Known wobble uridine modifications in yeast. (*B*) The ALKBH8 reaction mechanism. The MTase domain of ALKBH8 together with the cofactor TRMT112 uses S-adenosyl-L-methionine (SAM) to convert cm^{5}U into mcm^{5}U. In the case of tRNA^{Gly}(UCC), the AlkB-like domain subsequently performs hydroxylation into (S)-mchm^{5}U.

5-methoxycarbonylmethyluridine (mcm^{5}U) and 5-methoxycarbonylmethyl-2-thiouridine (mcm^{5}s^{2}U), respectively (Kalhor and Clarke 2003; Fu et al. 2010a; Songe-Moller et al. 2010). The other modifications found on wobble uridines together with mcm^5 are 2-thiolation and 2′-O-methylation. Ncs2/Ncs6 catalyze the 2-thiolation of uridine (Huang et al. 2008; Nakai et al. 2008; Leidel et al. 2009; Noma et al. 2009). Its level declined in the Elongator and Trm9 mutants (Nakai et al. 2008; Noma et al. 2009). Trm7/Trm734 methylate the 2′-O of ribose in tRNA^{Leu}(ncm^{5}UmAA) (Pintard 2002; Guy et al. 2012). This ribose modification appears to be independent of base modifications, since Um could be found in wild type cells, and tRNA^{Leu}(ncm^{5}UAA) could be found in Trm7 deletion mutants (Guy et al. 2012). Carbamoylmethyl (ncm^5) modification has also been identified on wobble uridines, particularly in mutants with defective Trm9 (Johansson et al. 2008; Chen et al. 2011). The enzyme responsible for the conversion to ncm^5 has not been uncovered and it is unclear whether this modification represents an alternative pathway or a step preceding the conversion to mcm^5. However, in *Arabidopsis* mutants depleted of AtTRM9, the level of ncm^5 corresponded to the level in wild type (Leihne et al. 2011). This suggests that some pathways to the formation of these modifications might be distinctive for plants.

The human AlkB homolog (ALKBH) family includes nine enzymes—ALKBH1 to ALKBH8 (Wei et al. 1996; Duncan et al. 2002; Aas et al. 2003; Tsujikawa et al. 2007) and FTO (Gerken et al. 2007). Among them, ALKBH8 is the ortholog of Trm9 through its carboxy-terminal methyltransferase (MTase) domain (Fu et al. 2010a; Songe-Moller et al. 2010). The MTase domain requires the cofactor TRMT112 to catalyze wobble uridine methylation (Fu et al. 2010a; Songe-Moller et al. 2010). ALKBH8 contains two additional domains, the central AlkB-like domain that is common for the ABH family, and the amino-terminal RNA recognition motif (RRM) (Supplemental Fig. S1B; Pastore et al. 2012).

Studies of human ALKBH8 tRNA targets have been largely directed by data available from yeast studies. However, modifications in human tRNAs may differ from yeast modifications. For example, human tRNA^{Arg}(UCU) was found to contain mcm^{5}s^2 in contrast to mcm^5 in yeast (Songe-Moller et al. 2010), and the stop codon-recoding tRNA^{Sec}(UCA) is present in two subgroups of wobble modification: mcm^{5}U and mcm^{5}Um (Songe-Moller et al. 2010). Furthermore, the AlkB-like domain of ALKBH8 was shown to hydroxylate mcm^{5}U to (S)-methoxycarbonylhydroxymethyluridine [(S)-mchm^{5}U] in tRNA^{Gly}(UCC) (Fig. 1B; Fu et al. 2010b; van den Born et al. 2011). Its diastereomer (R)-mchm^{5}U is present in tRNA^{Arg}(UCG), but it remains unclear which enzyme mediates this hydroxylation.

The significance of ALKBH8 is supported by studies that reported its dysregulation in many types of cancers (Shimada et al. 2009; Begley et al. 2013; Ohshio et al. 2016, Feng et al. 2022). Moreover, the impairment of its catalytic function by loss-of-function or missense mutations in the carboxy-terminal region was associated with intellectual disability (Monies et al. 2019; Saad et al. 2021; Maddirevula et al. 2022; Waqas et al. 2022). To date, ALKBH8 RNA binding and enzymatic activity have been demonstrated in the following specifically selected tRNAs, tRNA^{Arg}(UCU), tRNA^{Gln}(UUG), tRNA^{Glu}(UUC), tRNA^{Sec}(UCA), tRNA^{Gly}(UCC), and tRNA^{Lys}(UUU) (Lu et al. 2005; Fu et al. 2010a,b; Songe-Moller et al. 2010; van den Born et al. 2011; Lentini et al. 2018). Other wobble U–containing tRNAs and other RNA species have not been addressed to date. In this study, we present an unbiased study of human ALKBH8 RNA targets by using high-throughput sequencing of crosslinked and immunoprecipitated RNAs (HITS-CLIP). Our results reveal the previously characterized tRNAs as well as several other tRNAs. Interestingly, the study also suggests binding of ALKBH8 to several other types of RNA.

RESULTS AND DISCUSSION

Identification of ALKBH8 targets by HITS-CLIP

To identify ALKBH8 RNA targets, we performed the HITS-CLIP analysis (Ule et al. 2005; König et al. 2010; Bartosovic et al. 2017). We first prepared a stable cell line of HEK293 T-Rex Flp-In (293T) with inducible expression of amino-terminally tagged ALKBH8 (FLAG-ALKBH8) (Fig. 2A). Both, the FLAG-ALKBH8 and endogenous ALKBH8 exhibited cytoplasmic localization (Fig. 2B,C), which is in agreement with the previously reported localization of episomally expressed GFP-ALKBH8 (Fu et al. 2010a; Pastore et al. 2012). FLAG-ALKBH8 formed strong protein–RNA complexes after UV irradiation (Fig. 2D). We performed three independent HITS-CLIP experiments. The bioinformatic analysis resulted in 15,798,568 uniquely mapped reads to the human genome (see Materials and Methods for details). As expected, annotation of mapped reads revealed tRNAs as the most prevalent target (87% of reads), followed by mRNA exons (7%), mRNA introns (3%), repetitive elements (1%), snoRNAs (0.2%) and snRNAs, miRNA and rRNA (all <0.1%) (Fig. 2E; Supplemental Table S2).

ALKBH8 targets a wider repertoire of U_{34}-containing tRNAs

The list of previously reported and validated mammalian ALKBH8 substrates included $tRNA^{Arg}$(UCU), $tRNA^{Gln}$(UUG), $tRNA^{Glu}$(UUC), $tRNA^{Sec}$(UCA), $tRNA^{Gly}$(UCC) and $tRNA^{Lys}$(UUU) (Lu et al. 2005; Fu et al. 2010a,b; Songe-Moller et al. 2010; van den Born et al. 2011, Lentini et al. 2018; Fig. 3A, top left; Fu et al. 2010a,b; Songe-Moller et al. 2010; van den Born et al. 2011). Our analysis identified additional tRNAs containing U at position 34 that were not previously reported as ALKBH8 targets in mammals (Fig. 3A, top right, Supplemental Table S2). These are $tRNA^{Leu}$(UAA), $tRNA^{Leu}$(UAG), and $tRNA^{Val}$(UAC). In yeast, $tRNA^{Leu}$(UAA) and $tRNA^{Val}$(UAC) contain ncm^5 modification for which the responsible enzymatic activities have not yet been identified (Randerath et al. 1979; Kalhor and Clarke 2003; Johansson et al. 2008). No wobble U modification has been reported for yeast $tRNA^{Leu}$(UAG).

To verify the HITS-CLIP results on a larger scale, we performed an ALKBH8 RNA immunoprecipitation and sequencing (RIP-seq) analysis. We analyzed RNAs coprecipitating with FLAG-ALKBH8 (RIP) without stabilization of the binding by crosslinking (Supplemental Fig. S1C). Tagged ALKBH8 was immunopurified with FLAG antibody, The advantage of this experiment is the absence of RNaseI treatment, which retains information about the full length of the bound small RNAs. We obtained 5,063,455 uniquely mapped reads under strict mapping conditions (one mismatch allowed). The annotation of the mapped reads revealed a high overlap with the HITS-CLIP data. The most enriched coprecipitated tRNAs included $tRNA^{Arg}$(UCU), $tRNA^{Gln}$(UUG), $tRNA^{Glu}$(UUC), $tRNA^{Gly}$(UCC), $tRNA^{Lys}$(UUU), and $tRNA^{Sec}$(UCA) (Fig. 3A, in gray; Supplemental Table S2). Another U_{34}-containing tRNA identified was $tRNA^{Val}$(UAC) (Supplemental Table S2).

The HITS-CLIP analysis also identified tRNAs with residues other than U at position 34. These include $tRNA^{Ala}$(AGC), $tRNA^{Arg}$(ACG), $tRNA^{Val}$(AAC), $tRNA^{Asp}$(GUC), $tRNA^{Gly}$(GCC), $tRNA^{His}$(GUG), $tRNA^{Phe}$(GAA), $tRNA^{Gln}$(CUG), $tRNA^{Glu}$(CUC), $tRNA^{Gly}$(CCC), $tRNA^{Leu}$(CAA), $tRNA^{Lys}$(CUU), $tRNA^{Ser}$(CGA), and $tRNA^{Val}$(CAC) (Fig. 3A; Supplemental Table S2). Some of them were also present in the RIP-seq data set: $tRNA^{Asp}$(GUC), $tRNA^{Gly}$(GCC), $tRNA^{His}$(GUG), $tRNA^{Gln}$(CUG), $tRNA^{Glu}$(CUC), $tRNA^{Gly}$(CCC), and $tRNA^{Lys}$(CUU).

Our analyses identified a number of tRNAs containing C at position 34. To further validate ALKBH8 binding to tRNAs with C versus U at the wobble position, we analyzed RNAs from ALKBH8 RIP by northern blot. Two wobble C tRNAs were chosen, $tRNA^{Lys}$(CUU) that appeared among CLIP targets (Fig. 3A) but was previously reported as a non-target (Fu et al. 2010a), and $tRNA^{Gly}$(CCC) that also appeared among CLIP targets and does not contain any uridines in the anticodon. Northern blot analysis revealed a strong signal for $tRNA^{Glu}$(UUC) and a weaker signal for $tRNA^{Lys}$(UUU) in the ALKBH8 RIP eluate (Fig. 3B). This agrees with the results of the HITS-CLIP, where $tRNA^{Glu}$(UUC) was among the most prominent targets, while $tRNA^{Lys}$(UUU) had ten times lower coverage (Supplemental Table S2). No signal was detected for tRNAs with C at the wobble codon position (Fig. 3B).

The HITS-CLIP analysis revealed a larger spectrum of tRNAs bound to ALKBH8, including tRNAs with nucleotides other than U at the wobble position. Such binding was also uncovered by RIP-seq, although in this case the tRNAs without wobble uridine were less represented than the wobble uridine–containing tRNAs (Supplemental Table S2). Noticeably, *tRNA-Glu-CUC-1-1* was detected with high counts per million (CPM) also by non-crosslinked RIP. Therefore, to verify modification status of tRNAs, we purified $tRNA^{Lys}$(UUU) and $tRNA^{Glu}$(CUC) from HEK293T and subjected them to liquid chromatography–mass spectrometry (LC–MS) analysis. $tRNA^{Lys}$(UUU) had been showed to contain wobble modification mcm^5s_2U by methods other than MS (Raba et al. 1979; Hedgcoth et al. 1984; Lu et al. 2005; Lentini et al. 2018). Our analysis revealed the presence of mcm^5s^2U and mcm^5U in $tRNA^{Lys}$(UUU) (Supplemental Fig. S2). On the contrary, the LC–MS analysis did not detect mcm^5U nor other marks resulting from ALKBH8 activity in $tRNA^{Glu}$(CUC). This tRNA manifests up to 97% identity with $tRNA^{Glu}$(UUC), which is a difference of only 2 nt. One of these two nucleotides is located in the D arm, and the other nucleotide is in the anticodon. An error in mapping to $tRNA^{Glu}$(CUC) was excluded by allowing the maximum mismatch of one nucleotide in the

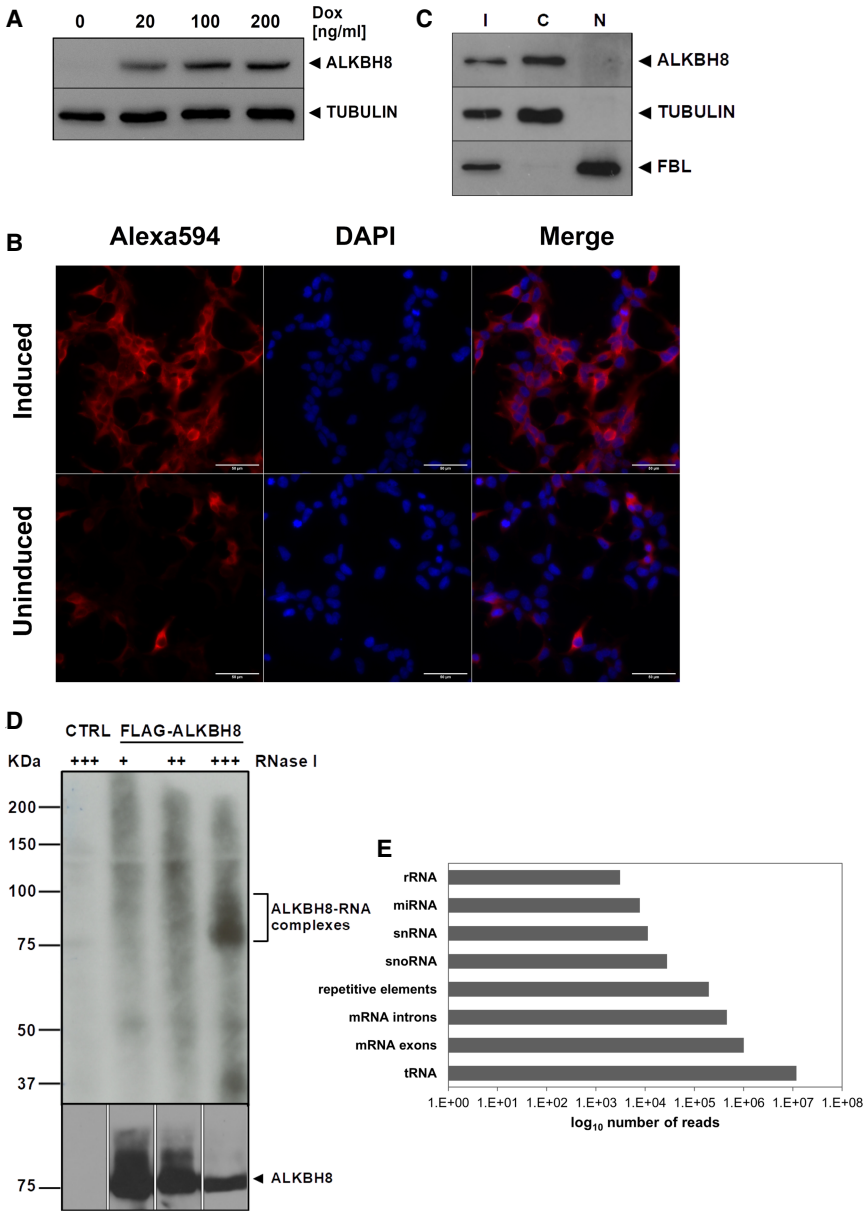

FIGURE 2. HITS-CLIP analysis of ALKBH8 RNA targets in HEK293 T-Rex Flp-In cells identifies a broader RNA binding repertoire. (*A*) Western blot analysis of the doxycycline-inducible expression of stably integrated 3x FLAG-ALKBH8. Tubulin was used as a loading control. (*B*) FLAG-ALKBH8 localizes in the cytoplasm in HEK293T. Immunofluorescence of FLAG-ALKBH8 whose expression was induced by doxycycline and visualized by anti-FLAG and Alexa594 antibodies (red). DNA was stained with DAPI (blue). The scale bar represents 50 µm. (*C*) ALKBH8 is present mainly in the cytoplasm. Western blot analysis of the total cell lysate (I), cytoplasmic (C), and nuclear (N) fractions of HEK293T cells. ALKBH8 was detected with a specific antibody. Tubulin was used as a cytoplasmic marker and fibrillarin (FBL) as a nuclear marker. (*D*) ALKBH8-RNA complexes formed by UV treatment. Cellular lysates were treated with an increasing concentration of RNaseI (marked *above* the gel). CTRL was a negative control of HEK293T in which FLAG-ALKB8 was not expressed. ALKBH8 was immunoprecipitated with anti-FLAG antibody. RNA was 5′-terminally labeled with γ^{32}P-ATP, and complexes were resolved on polyacrylamide and SDS-PAGE denaturing gels, respectively. The *upper* panel displays the radioactive signal of the RNA detected by autoradiography, and the *lower* panel is a western blot analysis with anti-FLAG antibody. (*E*) RNA classes identified by ALKBH8 HITS-CLIP experiments. The graph shows numbers of uniquely mapped reads (*x*-scale).

whole read and by using only uniquely mapped reads. Therefore, it is probable that ALKBH8 binds both tRNA^{Glu}(UUC) and tRNA^{Glu}(CUC) with high affinity in vivo due to their high sequence identity. The activity of ALKBH8 would then depend on the prior formation of the cm^{5}U modification (Kalhor and Clarke 2003).

ALKBH8 binds to mature tRNAs

tRNAs are produced as precursors with 5′- and 3′- trailers that are endonucleolytically cleaved by RNase P and tRNase Z (Guerrier-Takada et al. 1983; Schiffer et al. 2002) and 3′ termini are extended with CCA tails that the CCA nucleotidyltransferase adds (Rossmanith et al. 1995). Upon export to the cytoplasm, tRNA is charged with the corresponding aminoacid (Hampel and Enger 1973). Individual internal chemical modifications occur at different steps of tRNA processing. For instance, wybutosine formation at position 37 in yeast is catalyzed after retrograde import to the nucleus after nuclear intron removal in the cytoplasm (Yoshihisa et al. 2007; Ohira and Suzuki 2011). The timing of ALKBH8 activity and possible coordination with other processes is not yet fully understood. Furthermore, only limited information is available on the molecular principles of ALKBH8 RNA specificity and binding, as there is only the structure of the human RRM domain and the AlkB-like domain in complex with an oligonucleotide (Pastore et al. 2012). Therefore, we analyzed the properties of ALKBH8 binding to tRNAs in greater detail, as revealed by the HITS-CLIP. We plotted the CLIP coverage of highly covered tRNA targets on their genomic loci to display the sites of interaction with ALKBH8. Both wobble U and non-wobble U tRNAs exhibited a predominant signal over the 5′-half of the tRNA sequences (Fig. 3C,D). tRNA^{Gly}(UCC) was excluded from Figure 3C due to its strong coverage that masked the read distribution of less covered tRNAs. The

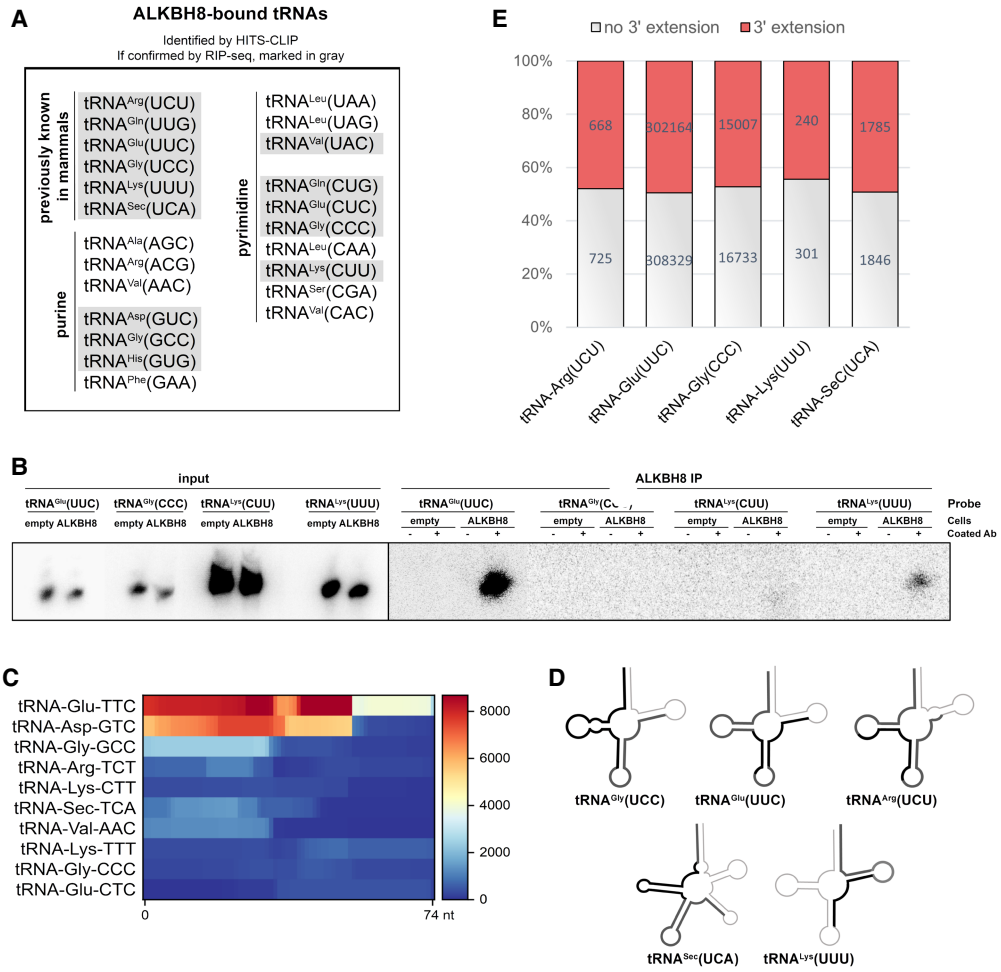

FIGURE 3. Analysis of ALKBH8-bound tRNAs identified by HITS-CLIP. (*A*) List of tRNAs identified by HITS-CLIP. The displayed tRNAs are the top-scoring tRNAs according to the CPM in Supplemental Table S2. The tRNAs also observed by ALKBH8 RIP-seq analysis are highlighted in gray. The first column (*top left*) are the previously known ALKBH8 tRNA targets. tRNAs are displayed according to the identity of the wobble nucleotide. (*B*) Northern blot analysis of selected tRNAs coprecipitated with ALKBH8. Empty are HEK293T cells without the integrated FLAG-ALKBH8 gene. ALKBH8 are stable cell lines that express FLAG-ALKBH8. Input is RNA isolated from whole cell extracts. ALKBH8 IP are RNAs coprecipitated with affinity-purified ALKBH8. Beads lacking anti-FLAG antibody were used as a control for nonspecific binding of tRNA (–). FLAG-coupled beads are marked as +. DNA oligo probes for individual tRNAs were 5′ terminal labeled by γ^{32}P-ATP. The RNAs were resolved on 20% polyacrylamide gel and the radioactive signals detected by autoradiography. (*C*) Heatmap representation of ALKBH8 binding to tRNAs as revealed by the HITS-CLIP analysis. The strong signal of tRNA-Gly-TCC was omitted in order to decrease the scale of the heat plot. All gene lengths were scaled to an equal length of 74 nt on the *x*-axis. The color scale on the *right* represents the CPM normalized number of mapped reads to a region. (*D*) Schematic representation of ALKBH8 binding to the secondary structure of tRNA. The areas with the highest mapping are highlighted by a thick black line, and the lower number of mapped reads is marked in thick gray. (*E*) Proportions of CPM normalized values of nontemplated 3′-terminal extensions in most represented tRNAs detected by RIP-seq. The red bars include all the different versions of 3′ extensions (C, CC, CCA, see details in Supplemental Fig. S1D). The number of tRNA reads without any nontemplated 3′-terminal extensions are in gray.

reads for the known targets tRNA^{Gly}(UCC), tRNA^{Glu}(UUC), and tRNA^{Arg}(UCU) mapping were extended over the anticodon loop toward the T-arm. The two tRNAs with predominant binding in the tRNA 3′ half were tRNA^{Lys}(UUU) and tRNA^{Glu}(CUC). The genes of tRNA^{Arg}(UCU) contain a 14-nt intron located downstream of position 37 that formed a signal gap in the read mapping to the genomic locus. Even though we are limited to only one example of an intron-containing tRNA, this finding suggested that ALKBH8 targets mature, fully spliced tRNAs.

Since the HITS-CLIP protocol involves RNA cleavage, we investigated the RIP-seq results that preserved the bound full-length tRNA, to inspect the tRNA termini. In particular, we analyzed the status of the 3′-terminal nontemplated addition of CCA. 50% of the reads that mapped to the known tRNA targets possessed the nontemplated nucleotide addition (Fig. 3E). These additions were generally composed of one or two nontemplated cytidines (Supplemental Fig. S1D). Twenty-two percent of the tRNA reads contained the mature CCA 3′-terminus.

tRNA^{Sec}(UCA) showed a different distribution of 3′-additions, where the CCA trinucleotide formed 70% of all additions (Supplemental Fig. S1D). However, the overall proportion of reads lacking any nontemplated 3′-terminus is in contrast to the consensus that tRNA nuclear export occurs only after the CCA addition. The relative affinity of tRNA for exportin-t/RangGTP is 10 times lower when tRNA is without 3′-CCA, and six times weaker when tRNA carries only 3′-CC (Lipowsky et al. 1999). Therefore, ALKBH8 might bind to tRNAs lacking 3′-CCA due to the activity of ANKZF1 and ELAC1 (Yip et al. 2019, 2020). The incomplete CCA termini are repaired by a cytosolic population of CCA-transferase (Wolfe et al. 1996). However, we cannot rule out the possibility that the CCA extensions might have been lost during the RIP protocol due to 3′ to 5′ exoribonucleolytic activities in the cell lysate.

ALKBH8 binds to other types of RNA in vivo

The highest scoring hits in the HITS-CLIP data sets also included other types of RNA (Supplemental Table S2). We identified a number of C/D box snoRNAs, for example, *SNORD13*, *SNORD16*, *SNORD18A*, *SNORD18C*, *SNORD26*, *SNORD34*, *SNORD42B*, *SNORD43*, *SNORD58C*, *SNORD72*, *SNORD83A*, and *SNORD83B* (Fig. 4A; Supplemental Table S2). In addition to snoRNAs, binding to other ncRNAs was found, such as *7SK RNA*, *RNY5*, the RNA component of vault particles *VTRNA1-2*, *miR186*, and *miR374A*. (Fig. 4A; Supplemental Table S2). Many reads were mapped to exonic and intronic regions of protein-coding genes even under highly strict mapping conditions (no or only one mismatch). In all cases, these mRNAs contained a single well-defined peak of 20 to 60 nt in length, which is narrower than the peaks in other classes of RNA (Supplemental Table S2). Further studies will tackle the question of whether ALKBH8 binding to these regions has any functional significance.

The RIP-seq data set included a high number of C/D box snoRNAs (Supplemental Table S2). Comparison of the results of HITS-CLIP and RIP-seq revealed an overlapping set of intron-encoded C/D box snoRNAs (*SNORD18A*, *SNORD18C*, *SNORD34*, *SNORD42B*, *SNORD43*, *SNORD58C*, *SNORD72*, *SNORD83A*, and *SNORD83B*) and other ncRNAs (*miR186*, *miR374A*, *7SK RNA*, *RNY5*) (Fig. 4A, in gray). Another set of C/D box snoRNAs showed high CPM only in the RIP data set, for example, *SNORD63*, *SNORD101*, *SNORD117*, *SNORD118* (Supplemental Table S2). To further validate ALKBH8 binding to non-tRNA targets, we analyzed RNAs from ALKBH8 RIP by reverse transcription-PCR (RT-PCR). We obtained signal for *SNORD18C*, *SNORD34*, *RN7SK*, and *VTRNA1-2* in the RNA coprecipitate from ALKBH8 RIP (Fig. 4C).

ALKBH8 is localized in the cytoplasm (Fig. 2C,E) as other anticodon loop-modifying enzymes such as FTSJ1, the human ortholog of 2′-O-methylase Trm7 (Li et al. 2020), or the U_{31}-specific pseudouridylase Pus6 (Ansmant et al. 2001). The Elongator, whose activity precedes ALKBH8 on wobble uridines, localizes principally in the cytoplasm and partially in the nucleus (Kim et al. 2002; Pokholok et al. 2002). Despite the location of ALKBH8, there is a striking representation of nuclear C/D box snoRNAs among the identified targets. However, their prominent nucleolar location is not exclusive. *U3 snoRNA* is known to shuttle between the nucleus and the cytoplasm (Leary et al. 2004) and has been reported to be processed into functional miRNAs (Lemus-Diaz et al. 2020). Other snoRNAs were observed in the cytoplasm after oxidative stress (Holley et al. 2015). ALKBH8 is involved in the response to oxidative stress by enhancing the translation of detoxification enzymes containing selenocysteine by catalyzing the modification of tRNA^{Sec}(UCA) (Endres et al. 2015a). The partial cytoplasmic localization of snoRNAs in *Arabidopsis thaliana* under physiological conditions (Streit et al. 2020) indicates a possible cytoplasmic distribution also in other organisms.

Another possible link to ALKBH8 binding to snoRNAs may be the finding that some snoRNAs show activity on tRNAs. For example, human *SNORD97* together with *SCARNA97* catalyzes 2′-O-methylation of C_{34} of tRNA^{Met}(CAU) (Vitali and Kiss 2019). PAR-CLIP performed on the FBL, NOP56, NOP58, and DKC1 snoRNP proteins showed a small fraction of bound tRNAs (Kishore et al. 2013). It is possible that ALKBH8 and snoRNAs simultaneously interact with tRNA, leading to binding signals in the HITS-CLIP data.

Wobble uridine-like modifications that are known to be catalyzed by ALKBH8 have not been found in other RNA species (Cantara et al. 2011; Boccaletto et al. 2018). However, to our knowledge, mcm^{5}U/mchm^{5}U has not been examined in detail in a wide range of RNAs. There are enzymes known to have dual specificity on distinct RNA species. For instance, NSUN2 introduces 5-methylcytosine to tRNA at position C_{34} (Brzezicha et al. 2006; Auxilien et al. 2012) and to vault RNAs (Hussain et al. 2013). Furthermore, fluorescence anisotropy assays showed unspecific binding of the ALKBH8/TRMT112 complex to a 17mer composed of random nucleotides with the dissociation constant 350 ± 20 nM (Pastore et al. 2012). This value represents an affinity similar to binding a 17-nt stem–loop derived from a tRNA^{Gly} target that had the dissociation constant of 240 ± 29 nM or to an ALKBH8 aptamer that demonstrated a dissociation constant of 240 ± 50 nM. This supports the hypothesis that ALKBH8 binds and possibly modifies other substrates than tRNA in vivo.

Other ncRNAs, namely vault RNA, Y RNA and *7SK RNA*, that were identified in our HITS-CLIP data, had previously been identified in other CLIP-seq experiments with the RNA modifier enzymes Pus7 pseudouridinylase (Guzzi

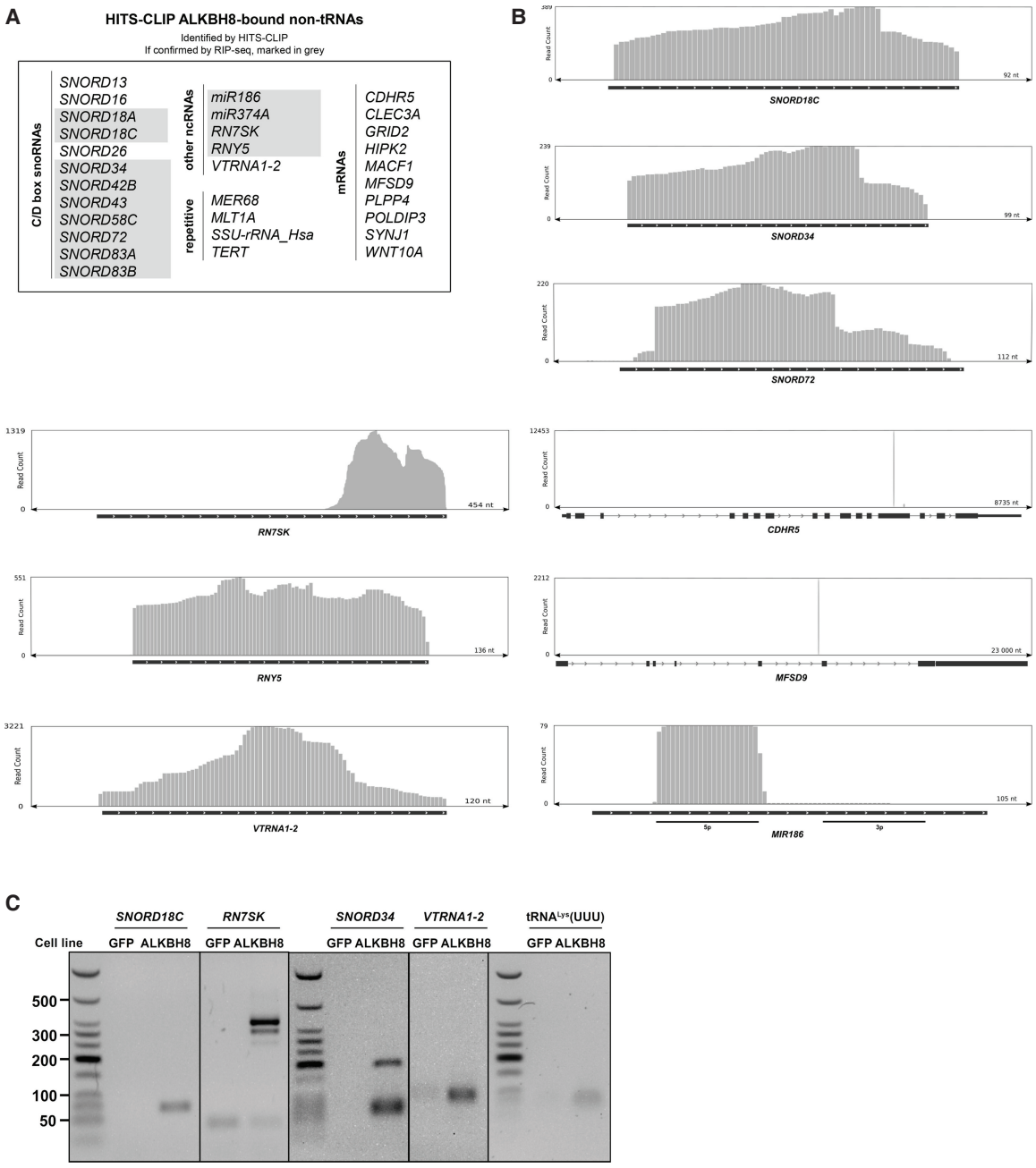

FIGURE 4. HITS-CLIP analysis of ALKBH8 revealed non-tRNA types of RNA. (*A*) Top-scoring bound RNAs according to CPM (Supplemental Table S2). Targets that were recapitulated by RIP-seq analysis are colored gray. Genes are listed in numerical and alphabetical order. (*B*) Representation of ALKBH8 binding to selected genomic regions of RNA. (*C*) RT-PCR analysis of selected RNAs coprecipitated with ALKBH8. GFP is the control HEK293T cell line that expresses FLAG-GFP. ALKBH8 is the HEK293T stable cell line that expresses FLAG-ALKBH8. The coprecipitated RNA was reverse transcribed, the targets were amplified using gene-specific primers, and the amplicons were resolved on agarose gel. The faster migrating bands in the 7SK panel correspond to the primer-dimer signal. The slower migrating PCR product in the *SNORD34* panel is an unspecific PCR product.

et al. 2018), METTL16 N^6-adenosine methyltransferase (Warda et al. 2017) or Nsun2 5-methylcytosine transferase (Hussain et al. 2013). Interestingly, Y RNAs were discovered to be modified with N-glycans (Flynn et al. 2021). Substantial research is needed to reveal all the modifications that are likely present in these RNAs.

The presence of mRNAs in the HITS-CLIP data set was surprising. In recent years, much research has focused on mRNA modifications. The modifications discovered are located in both coding and noncoding mRNA regions. These modifications tend to be simple methylations, although more bulky modifications such as 5-

hydroxymethylcytidine or N^6-acetylcytidine have also been identified (Fu et al. 2014; Arango et al. 2018; Anreiter et al. 2020). The only known uridine modification on mRNA is pseudouridine (Safra et al. 2017). Despite the growing understanding of the variety of mRNA modifications, it seems rather unlikely that ALKBH8 would exhibit its catalytic activity on protein-coding genes. Nevertheless, the mRNAs identified by HITS-CLIP had high read counts and displayed one or two sharp peaks. At the moment, the significance of these data remains enigmatic.

To test whether ALKBH8 displays sequence preference, we performed a motif analysis for both tRNAs and non-tRNA classes identified by the HITS-CLIP (Supplemental Fig. S4A,B, respectively). Interestingly, both categories revealed UAGUG, GUCUA, GUGGU, AUAGC, and AGUGG as the most abundant pentamers (Supplemental Fig. S4C).

It is conceivable that binding of ALKBH8 to other tRNAs may have additional functional consequences. TRMT9B (also known as hTRM9L) is the human paralog of ALKBH8. In contrast to ALKBH8, it contains solely the MTase domain. Interestingly, it is a phosphoprotein that has been shown to act during oxidative stress in MEK-ERK-RSK signaling (Gu et al. 2018). This supports the idea that ALKBH8 might also act in a manner independent of its catalytic function. Nevertheless, we cannot exclude the possibility that the overexpressed ALKBH8 might have resulted in nonspecific interactions with a wide set of RNAs that do not present functional relevance.

Taken together, our results confirmed that ALKBH8 primarily targets mature, CCA modified tRNAs that contain wobble uridine. The HITS-CLIP and RIP-seq results further revealed binding to a broader RNA repertoire, such as C/D box snoRNAs, 7SK or vault RNAs. Further studies will reveal the functional relevance of these interactions.

MATERIALS AND METHODS

Preparation of the FLAG-ALKBH8 expression construct

The synthetic sequence of the 3x FLAG tag (Supplemental Table S1) was inserted between the KpnI and NotI sites of the vector pcDNA5/FRT/TO (ThermoFisher Scientific) to prepare a DNA construct for amino-terminal FLAG fusions. The full-length (1994 bp) *ALKBH8* coding region was amplified using primers ALKBH8_fwd and ALKBH8_rev (Supplemental Table S1). As a template for PCR, we used oligo dT-primed cDNA synthesized from total RNA isolated from HEK293 T-Rex Flp-In cells. The PCR product was inserted between the NotI and XhoI sites of pcDNA5/FRT/TO/FLAG to obtain the amino-terminal 3x FLAG fusion gene. The final construct was verified by sequencing.

Cell culture and stable cell line preparation

Human embryonic kidney (HEK293) T-Rex Flp-In (Thermo Fisher Scientific) cells were grown in DMEM supplemented with 10% FBS in an atmosphere of 5% CO2, 37°C. At 70% confluency, cells were cotransfected with 1 µg of pcDNA5/FRT/TO/3xFLAG-ALKBH8 and 10 µg of pOG44 using TurboFect Transfection Reagent (Thermo Fisher Scientific). After 24 h, cells were transferred to a 15-cm dish and recombinants were selected in the presence of 100 µg/mL of hygromycin B. When individual cell colonies were grown, the colonies were tested for doxycycline-inducible expression of 3x FLAG-ALKBH8 and zeocin sensitivity.

Western blot

Proteins were resolved by SDS-PAGE and transferred to a nitrocellulose membrane. Primary antibodies used in this study are: anti-FLAG (1:3000, Sigma Aldrich F3165), anti-tubulin (1:10,000, Sigma Aldrich T6074), anti-fibrillarin (1:1000, Abcam ab5821), anti-ALKBH8 (1:500, Abcam ab113512). Washes and incubation of HRP-conjugated secondary antibodies (1:5000, Promega) were performed in PBST (0.05% Tween 20 in PBS). Pierce ECL Western Blot Substrate (Thermo Fisher Scientific) was used for visualization.

Immunofluorescence

Cells grown on polyethyleneimine-coated coverslips were fixed with 3.7% paraformaldehyde for 30 min and permeabilized with 0.2% Triton X-100 in PBS for 20 min. One hour of blocking with 5% horse serum in PBS was followed by incubation with anti-FLAG primary antibody (1:500, Sigma Aldrich F3165) in 3% horse serum in PBS for 1 h. Alexa594 secondary antibody (1:1000, Invitrogen A-21203) incubation was performed together with DAPI (1:500, Sigma) in 3% horse serum in PBS for 30 min. All washes were performed in PBS and the final wash was in PBST. Coverslips were mounted on microscopy slides in Mowiol 4-88 (Sigma) with DABCO. The imaging for the localization overview was performed on the Zeiss AxioImager.Z2-Zen upright fluorescence microscope with the objective Plan-Apochromat 63×/1.40 Oil.

Subcellular fractionation

Subcellular fractionation was performed as previously published (Ustianenko et al. 2016). Briefly, HEK293 T-Rex Flp-In cells were permeabilized in the dish with digitonin (45 µg/mL digitonin, 10 mM DTT, 10 mM $MgCl_2$ in 1× NEH buffer). The released cytoplasmic fraction was collected and cleared by centrifugation. Cell residues in the dish were scraped in buffer 2 (150 mM NaCl, 1% NP-40, 50 mM HEPES pH 7.4). The nuclear fraction was harvested by centrifugation.

HITS-CLIP protocol

HITS-CLIP was performed in triplicates as previously described in Bartosovic et al. (2017). Briefly, cells induced with 0.1 mg/mL of doxycycline were UV-crosslinked (150 mJ/cm at 254 nm) and lysed in 100 mM NaCl, 50 mM Tris pH 7.4, 1% NP-40, 0.1% SDS, 0.5% sodium deoxycholate, and 1× EDTA-free Complete Protease Inhibitor Cocktail (Roche). After brief sonication, the lysates were treated with Turbo DNase (Fermentas) and RNase I

(Ambion). Protein G Dynabeads (Thermo Fisher Scientific) were coupled with anti-FLAG antibody (Sigma) and used for the immunoprecipitation of FLAG-ALBH8 complexes. The beads were then washed with high salt buffer (lysis buffer with 1 M NaCl and 1 mM EDTA) and PNK buffer (20 mM Tris pH 7.4, 10 mM $MgCl_2$, 0.2% Tween 20). RNA was treated with Fast AP Thermosensitive Alkaline Phosphatase (Fermentas), and the L3 DNA linker (Supplemental Table S1) was ligated to RNA by T4 RNA Ligase 2 (NEB). The beads were washed with high salt buffer and PNK buffer. RNA was labeled with gamma-^{32}P-ATP using T4 PNK (NEB). After washing with PNK buffer, the elution from the beads was performed by incubation at 95°C for 5 min. The eluted protein–RNA complexes were resolved on a 4%–12% NuPage gel (Thermo Fisher Scientific), transferred to a nitrocellulose membrane (Bio-Rad) and the area corresponding to the migration of ALKBH8 and 20 kDa above was cut from the membrane. The membrane was cut into pieces and PK buffer (100 mM Tris pH 7.4, 50 mM NaCl, 10 mM EDTA) was added together with Proteinase K (NEB). After 90 min of incubation at 37°C, an equal volume of PK buffer with 7 M urea was added and RNA was extracted by incubation at 55°C for 1 h. RNA was purified by phenol/chloroform extraction and ethanol precipitation. The RNA linker L5 (Supplemental Table S1) was ligated with T4 RNA ligase (NEB). RNA was purified by phenol/chloroform extraction. SuperScript III (Thermo Fisher Scientific) and random hexamers were used for reverse transcription and PCR amplification was carried out using 25 cycles and GoTaq polymerase (Promega) with linker specific primers. The quality of the PCR libraries was analyzed by Bioanalyzer, and high-throughput sequencing was performed in the 75 bp single-end mode on Illumina HiSeq 2000 at the Vienna BioCenter (VBCF) Sequencing facility.

RNA immunoprecipitation and preparation of cDNA library (RIP-seq)

FLAG-ALKBH8 expression was induced with 0.1 mg/mL doxycycline at 70% confluency in two 10 cm plates. Eighteen hours later, cells were harvested, washed twice with 1× PBS, and lysed in 1.4 mL of lysis buffer (50 mM Tris pH 8.0, 150 mM NaCl, 1% Triton X-100, 1 mM DTT, 1× EDTA-free Complete Protease Inhibitor Cocktail [Roche] and 110 U/mL of RNasin [Promega]) rolling for 30 min at 5°C. The lysate was treated with 2 U/mL Turbo DNase (Fermentas) for 15 min at 37°C. The insoluble fraction was removed by centrifugation at 15,000*g* for 15 min, the supernatant was incubated with 1/14 volume of free Protein G Dynabeads (Thermo Fisher Scientific) rolling for 1 h at 5°C to remove sticky proteins and RNAs. The precleared lysate was then transferred to Protein G Dynabeads coupled with anti-FLAG antibody (Sigma) and the mixture was incubated for 2 h at 5°C on a roller. The beads with bound proteins were washed three times with 1 mL of lysis buffer. RNA was isolated using TriPure Isolation Reagent (Roche) according to the manufacturer's protocol, precipitated in an equal volume of isopropanol and 7.5 µg/mL of GlycoBlue (Ambion) at −20°C, washed with 1 mL of 85% ethanol and the pellets were resuspended in 10 µL H_2O.

The L3 DNA linker at 0.5 µM concentration (Supplemental Table S1) was ligated to RNA in a 20 µL reaction using 5 U/µL of RNA Ligase Truncated K227Q (NEB) in the presence of 15% PEG8000 and 1 U/µL RNasin (Promega) at 18°C overnight and then at room temperature for 1 h and inactivated at 65°C for 20 min. RNA was purified by phenol/chloroform extraction and ethanol precipitation and the pellets were resuspended in 6 µL H_2O. The L5 RNA linker at 1 µM concentration (Supplemental Table S1) was ligated to RNA in a 20 µL reaction using 1 U/ µL of RNA Ligase 1 (NEB) in the presence of 15% PEG8000, 1 U/µL RNasin (Promega) and 1 mM ATP at 16°C overnight. RNA was purified by phenol/chloroform extraction and ethanol precipitation. SuperScript IV (Invitrogen) was used for reverse transcription and the resulting cDNA was treated with 1.25 U/µL RNase H (Invitrogen). cDNAs were amplified by 15 PCR using GoTaq G2 polymerase (Promega) and TruSeq_adaptor_fwd and TruSeq_adaptor_rev primers (Supplemental Table S1). The PCR products were resolved on a 2% agarose gel and the fragments migrating within the range of 200 to 330 nt were excised and the DNA was extracted using the Gel Extraction Kit (Qiagen) according to the manufacturer's instructions. 125-bp pair-end sequencing was performed on Illumina HiSeq V4 PE125 at the Vienna BioCenter Core Facilities.

Reverse transcription (RT)-PCR

RNA isolated by RNA purification was reverse-transcribed by SuperScript IV (Invitrogen) and treated with 1.25 U/µL RNase H (Invitrogen). cDNA was amplified by PCR using GoTaq G2 polymerase (Promega), gene-specific primers (Supplemental Table S1) and optimized number of PCR cycles.

Northern blot analysis

RNA was separated on a 16% polyacrylamide gel and transferred to the Amersham Hybond-N+ membrane (GE Healthcare). Probes tRNA-Glu-TTC, tRNA-Lys-TTT, tRNA-Lys-CTT, and tRNA-Gly-CCC (Supplemental Table S1) were radioactively labeled with gamma-^{32}P-ATP using T4 PNK (NEB). Prehybridization and hybridization were performed in OligoHyb Buffer (Applied Biosystems) at 50°C. The membrane was washed twice with 300 mM NaCl, 30 mM tri-sodium citrate, 0.1% SDS, pH 7.0, and twice with 15 mM NaCl, 1.5 mM tri-sodium citrate, 0.1% SDS, pH 7.0. The radioactive signal was detected by autoradiography.

Bioinformatics analyses of high-throughput sequencing data

Sequencing quality control was performed with the FastQC tool (Andrews 2010) and preprocessing, including the removal of sequencing adapters, and the removal of low-quality reads ($Q < 25$) and bases was achieved with Trimmomatic (Bolger et al. 2014).

High quality reads were mapped to a high confidence tRNA data set obtained from GtRNAdb using the Smith-Waterman algorithm for optimal local alignment in R (ver. 3.6.3) and Biostrings package (ver. 2.52.0) with the following settings: pairwiseAlignment (target_seq, query_seq, type = "local," substitutionMatrix = nucleotideSubstitutionMatrix (match = 1, mismatch = −1), gapOpening = 10, gapExtension = 0.1). Only uniquely mapped reads that aligned at least in 66% of their length and had a maximum of three mismatches were used for later analyses.

Reads that did not map uniquely to this data set were mapped to the human genome version GRCh38.p12 by STAR (Dobin et al. 2013), a splice-aware mapping program using ENSEMBL recommended settings, with maximum intron size = 10 kb, 3 nt or 0.03% mismatches and allowed soft clipping. Uniquely mapped reads were identified using Samtools (Li et al. 2009), and CLIP reads were categorized and annotated according to the priority table (1. rRNA, 2. tRNA, 3. snoRNA, 4. snRNA, 5. miRNA, 6. mRNA exon, 7. mRNA intron, 8. lincRNA, 9. repetitive elements 10. antisense mRNA, 11. unannotated). In the next step, the genome with mapped reads was dissected into 10 bp windows and the coverage for each CLIP library was calculated using the bamcoverage utility from the Deeptools2 package (Ramírez et al. 2016). Data from both mapping to GtRNAdb and the human genome were normalized using the counts per million (CPM) method. Identification of the crosslinking site in HITS-CLIP data mapped to the human genome was performed with Piranha (Uren et al. 2012). To identify the highest probable targets of ALKBH8 in addition to tRNA, we have combined the results of annotation, coverage calculation, and peak calling using the intersectBed tool from the BEDtools suite (Quinlan and Hall 2010) and sorted them according to CPM and identified peaks. The heatmap showing the binding regions on selected tRNA target genes was generated using the Deeptools2 package with the scaled region set to 74 nucleotides. To identify the nontemplated 3′ CCA tails from RIP-seq data, the reads exploited were the first ones of the paired reads that mapped uniquely into genomic regions of selected tRNAs. The soft-clipped parts were extracted. The CPM normalized numbers of nontemplated 3′ tails and of sequences without any extension were counted using a custom Python script. We considered the sequences as containing nontemplated 3′ tails only when they were ending with C, CC, CA, CCC, CCA, CCAA, or CCACCA.

The findMotifs.pl of the HOMER (Heinz et al. 2010) toolset was used for motif detection and enrichment in our sequences used as the target set. The background set of sequences was generated by the tool by shuffling the target set. We instructed the tool to find only motifs of 5 to 10 nt in the RNA mode. An in-house script in R (R Core Team 2020) was used for the detection of all 5-mers in the tRNA and non-tRNA sequences to compare their enrichment/depletion in these two sets. Detection was performed as an exact match without mismatches and indels.

Purification of cellular $tRNA^{Lys}$(UUU) and $tRNA^{Glu}$(CUC)

$tRNA^{Lys}$(UUU) and $tRNA^{Glu}$(CUC) were purified according to (Drino et al. 2020). Briefly, total RNA was isolated from three 15 cm plates of HEK293T cells grown to 90% confluency using TRIzol and isopropanol precipitated. Small RNA fractions, containing tRNAs, were eluted in 40%–60% of IEX buffer B (20 mM Tris, 1 M NaCl, 10 mM KCl, 1.5 mM $MgCl_2$,). For ion exchange chromatography, a HiTrap Q FF anion exchange chromatography column (1 mL, GE Healthcare) was used on an ÄKTA-FPLC (GE Healthcare) at 4°C. Eluted fractions between 400–600 mM NaCl were collected and immediately precipitated using isopropanol at −20°C. Eluted small RNA fractions were pooled and resuspended in water, supplemented with 10 mM $MgCl_2$ and renatured by incubation at 75°C for three minutes, immediately cooled on ice and mixed with 20 mL of binding buffer (30 mM HEPES KOH, 1.2 M NaCl, 10 mM $MgCl_2$). For RNA affinity capture, 80 µg of a 5′ amino-modified DNA oligonucleotide (Supplemental Table S1) complementary to target tRNA (IDT) was covalently coupled to a HiTrapTM NHS-activated HP column (1 mL, GE Healthcare). Binding to the NHS column was performed by recirculation of the small RNA fraction over the complementary NHS columun for 3 h at 65°C. The columns were washed with wash buffer (2.5 mM HEPES KOH, 0.1 M NaCl, 10 mM $MgCl_2$) and tRNAs were eluted by submerging the column in a water bath at 75°C in elution buffer (0.5 mM HEPES-KOH, 1 mM EDTA), precipitated with isopropanol at −20°C and the pellets were resuspended in water. Purified tRNAs were further gel-purified (8% urea-PAGE in 0.5× TBE) using RNA gel extraction buffer (0.3 M NaOAc, pH 5.2, 0.1% [v/v] SDS, 1 mM EDTA) and immediately precipitated with isopropanol and resuspended in water.

Liquid chromatography–mass spectrometry (LC–MS/MS) analysis of tRNA modifications

LC–MS analysis was performed as described previously (Thüring et al. 2016). A total of 500 ng of RNA was digested to the nucleoside level using 0.6 U nuclease P1 from *P. citrinum* (Sigma-Aldrich), 0.2 U snake venom phosphodiesterase from *C. adamanteus* (Worthington), 0.2 U bovine intestine phosphatase (Sigma-Aldrich), 10 U benzonase (Sigma-Aldrich) and 200 ng Pentostatin (Sigma-Aldrich) in 5 mM Tris (pH 8) and 1 mM magnesium chloride for 2 h at 37°C. An amount of 450 ng of digested RNA was spiked with 50 ng of internal standard (^{13}C stable isotope-labeled nucleosides from *S. cerevisiae*) and analyzed by LC–MS (Agilent 1260 Infinity system in combination with an Agilent 6470 Triple Quadrupole mass spectrometer equipped with an electrospray ion source [ESI]). For HPLC separations, a C18 reverse HPLC column (Synergi 4 µM particle size, 80 Å pore size, 250 × 2.0 mm; Phenomenex) was used. A gradient solvent system consisting of solvent A (5 mM ammonium acetate buffer, pH 5.3, adjusted with acetic acid) and solvent B (LC–MS grade acetonitrile, Honeywell) was used and the compounds were eluted with a linear gradient of 0%–8% solvent B over 10 min, followed by 8%–40% solvent B over 10 min. Initial conditions were regenerated with 100% solvent A for 10 min. The flow rate was 0.35 mL/min and the separations were performed with the column temperature maintained at 35°C. The four main nucleosides were detected photometrically at 254 nm using a diode array detector (DAD). Electrospray ionization mass spectra were recorded in positive polarity at a gas temperature of 300°C, gas flow of 7 L/min, nebulizer pressure of 60 psi, sheath gas temperature of 400°C, sheath gas flow of 12 L/min and capillary voltage of 3000 V. Agilent MassHunter software was used in the dMRM (dynamic multiple reaction monitoring) mode.

DATA DEPOSITION

The high-throughput sequencing data sets were deposited in the NCBI under the number PRJNA678596.

SUPPLEMENTAL MATERIAL

Supplemental material is available for this article.

ACKNOWLEDGMENTS

We want to thank Karolina Vavrouskova for excellent technical support, Dasa Zigackova for help with cell fractionation and Hana Macickova Cahova for helpful advice on tRNA modifications. This work was supported by the Czech Science Foundation (19-21829S to S.V.; T.S. was supported by 20-19617S), the Ministry of Education, Youth and Sports within program INTER-COST (LTC18052) and the institutional support of CEITEC 2020 (LQ1601). M.B. was supported by Brno City Municipality Scholarship for Talented Ph.D. Students. We further acknowledge the CELLIM core facility supported by MEYS CR (LM2018129 Czech-BioImaging). Computational resources were provided by the project "e-Infrastruktura CZ" (e-INFRA LM2018140) provided within the program Projects of Large Research, Development, and Innovations Infrastructures.

Author contributions: M.B. and S.V. conceived the project. M.B. prepared vectors, stable cell lines and performed HITS-CLIP. I.C. performed I.F., W.B., R.I.P., and northern blot. T.S. and M.D. performed bioinformatics analyses. P.R. and A.D. purified tRNAs; M.C.S.-D. and M.H. performed LC–MS analyses. P.R. performed RT-PCR. I.C. and S.V. interpreted the results and wrote the manuscript. I.C. prepared the figures. S.V. supervised the project.

Received August 16, 2022; accepted September 9, 2022.

REFERENCES

Aas PA, Otterlei M, Falnes PØ, Vågbø CB, Skorpen F, Akbari M, Sundheim O, Bjørås M, Slupphaug G, Seeberg E, et al. 2003. Human and bacterial oxidative demethylases repair alkylation damage in both RNA and DNA. *Nature* **421:** 859–863. doi:10.1038/nature01363

Alkatib S, Scharff LB, Rogalski M, Fleischmann TT, Matthes A, Seeger S, Schöttler MA, Ruf S, Bock R. 2012. The contributions of wobbling and superwobbling to the reading of the genetic code. *PLoS Genet* **8:** e1003076. doi:10.1371/journal.pgen.1003076

Andrews S. 2010. Fast:QC: a quality control tool for high throughput sequence data. http://www.bioinformatics.babraham.ac.uk/projects/fastqc.

Anreiter I, Mir Q, Simpson JT, Janga SC, Soller M. 2020. New twists in detecting mRNA modification dynamics. *Trends Biotechnol* **39:** 72–89. doi:10.1016/j.tibtech.2020.06.002

Ansmant I, Motorin Y, Massenet S, Grosjean H, Branlant C. 2001. Identification and characterization of the tRNA: Ψ_{31}-synthase (Pus6p) of *Saccharomyces cerevisiae*. *J Biol Chem* **276:** 34934–34940. doi:10.1074/jbc.M103131200

Arango D, Sturgill D, Alhusaini N, Dillman AA, Sweet TJ, Hanson G, Hosogane M, Sinclair WR, Nanan KK, Mandler MD, et al. 2018. Acetylation of cytidine in mRNA promotes translation efficiency. *Cell* **175:** 1872–1886. doi:10.1016/j.cell.2018.10.030

Auxilien S, Guérineau V, Szweykowska-Kulińska Z, Golinelli-Pimpaneau B. 2012. The human tRNA m^5C methyltransferase Misu is multisite-specific. *RNA Biol* **9:** 1331–1338. doi:10.4161/rna.22180

Bartosovic M, Molares HC, Gregorova P, Hrossova D, Kudla G, Vanacova S. 2017. N6-methyladenosine demethylase FTO targets pre-mRNAs and regulates alternative splicing and 3′-end processing. *Nucleic Acids Res* **45:** 11356–11370. doi:10.1093/nar/gkx778

Begley U, Sosa MS, Avivar-Valderas A, Patil A, Endres L, Estrada Y, Chan CTY, Su D, Dedon PC, Aguirre-Ghiso JA, et al. 2013. A human tRNA methyltransferase 9-like protein prevents tumour growth by regulating LIN9 and HIF1-α. *EMBO Mol Med* **5:** 366–383. doi:10.1002/emmm.201201161

Boccaletto P, Machnicka MA, Purta E, Piątkowski P, Bagiński B, Wirecki TK, de Crécy-Lagard V, Ross R, Limbach PA, Kotter A, et al. 2018. MODOMICS: a database of RNA modification pathways. 2017 update. *Nucleic Acids Res* **46:** D303–D307. doi:10.1093/nar/gkx1030

Bolger AM, Lohse M, Usadel B. 2014. Trimmomatic: a flexible trimmer for Illumina sequence data. *Bioinformatics* **30:** 2114–2120. doi:10.1093/bioinformatics/btu170

Brzezicha B, Schmidt M, Makałowska I, Jarmołowski A, Pieńkowska J, Szweykowska-Kulińska Z. 2006. Identification of human tRNA:m^5C methyltransferase catalysing intron-dependent m^5C formation in the first position of the anticodon of the pre-$tRNA^{(CAA)}_{Leu}$. *Nucleic Acids Res* **34:** 6034–6043. doi:10.1093/nar/gkl765

Cantara WA, Crain PF, Rozenski J, McCloskey JA, Harris KA, Zhang X, Vendeix FAP, Fabris D, Agris PF. 2011. The RNA modification database, RNAMDB: 2011 update. *Nucleic Acids Res* **39:** D195–D201. doi:10.1093/nar/gkq1028

Chen C, Huang B, Anderson JT, Byström AS. 2011. Unexpected accumulation of ncm^5U and ncm^5s^2U in a *trm9* mutant suggests an additional step in the synthesis of mcm^5U and mcm^5s^2U. *PLoS One* **6:** e20783. doi:10.1371/journal.pone.0020783

Crick FHC. 1966. Codon—anticodon pairing: the wobble hypothesis. *J Mol Biol* **19:** 548–555. doi:10.1016/S0022-2836(66)80022-0

Dauden MI, Kosinski J, Kolaj-Robin O, Desfosses A, Ori A, Faux C, Hoffmann NA, Onuma OF, Breunig KD, Beck M, et al. 2017. Architecture of the yeast Elongator complex. *EMBO Rep* **18:** 264–279. doi:10.15252/embr.201643353

Dobin A, Davis CA, Schlesinger F, Drenkow J, Zaleski C, Jha S, Batut P, Chaisson M, Gingeras TR. 2013. STAR: ultrafast universal RNA-seq aligner. *Bioinformatics* **29:** 15–21. doi:10.1093/bioinformatics/bts635

Drino A, Oberbauer V, Troger C, Janisiw E, Anrather D, Hartl M, Kaiser S, Kellner S, Schaefer MR. 2020. Production and purification of endogenously modified tRNA-derived small RNAs. *RNA Biol* **17:** 1104–1115. doi:10.1080/15476286.2020.1733798

Duncan T, Trewick SC, Koivisto P, Bates PA, Lindahl T, Sedgwick B. 2002. Reversal of DNA alkylation damage by two human dioxygenases. *Proc Natl Acad Sci* **99:** 16660–16665. doi:10.1073/pnas.262589799

Endres L, Begley U, Clark R, Gu C, Dziergowska A, Małkiewicz A, Melendez JA, Dedon PC, Begley TJ. 2015a. Alkbh8 regulates selenocysteine-protein expression to protect against reactive oxygen species damage. *PLoS One* **10:** e0131335. doi:10.1371/journal.pone.0131335

Endres L, Dedon PC, Begley TJ. 2015b. Codon-biased translation can be regulated by wobble-base tRNA modification systems during cellular stress responses. *RNA Biol* **12:** 603–614. doi:10.1080/15476286.2015.1031947

Feng S, Xu Z, Peng J, Zhang M. 2022. The AlkB family: potential prognostic biomarkers and therapeutic targets in glioblastoma. *Front Oncol* **12:** 847821. doi:10.3389/fonc.2022.847821

Flynn RA, Pedram K, Malaker SA, Batista PJ, Smith BAH, Johnson AG, George BM, Majzoub K, Villalta PW, Carette JE, et al. 2021. Mammalian Y RNAs are modified at discrete guanosine residues with N-glycans. *Cell* **184:** 3109–3124. doi:10.1016/j.cell.2021.04.023

Fu D, Brophy JAN, Chan CTY, Atmore KA, Begley U, Paules RS, Dedon PC, Begley TJ, Samson LD. 2010a. Human AlkB homolog

ABH8 is a tRNA methyltransferase required for Wobble uridine modification and DNA damage survival. *Mol Cell Biol* **30:** 2449–2459. doi:10.1128/MCB.01604-09

Fu Y, Dai Q, Zhang W, Ren J, Pan T, He C. 2010b. The AlkB domain of mammalian ABH8 catalyzes hydroxylation of 5-methoxycarbonylmethyluridine at the Wobble position of tRNA. *Angew Chem Int Ed Engl* **49:** 8885–8888. doi:10.1002/anie.201001242

Fu L, Guerrero CR, Zhong N, Amato NJ, Liu Y, Liu S, Cai Q, Ji D, Jin S-G, Niedernhofer LJ, et al. 2014. Tet-mediated formation of 5-hydroxymethylcytosine in RNA. *J Am Chem Soc* **136:** 11582–11585. doi:10.1021/ja505305z

Gerken T, Girard CA, Tung Y-CL, Webby CJ, Saudek V, Hewitson KS, Yeo GSH, McDonough MA, Cunliffe S, McNeill LA, et al. 2007. The obesity-associated *FTO* gene encodes a 2-oxoglutarate-dependent nucleic acid demethylase. *Science* **318:** 1469–1472. doi:10.1126/science.1151710

Glasser A-L, El Adlouni C, Keith G, Sochacka E, Malkiewicz A, Santos M, Tuite MF, Desgrès J. 1992. Presence and coding properties of 2′-*O*-methyl-5-carbamoylmethyluridine (ncm^5Um) in the wobble position of the anticodon of $tRNA^{Leu}$ (U*AA) from brewer's yeast. *FEBS Lett* **314:** 381–385. doi:10.1016/0014-5793(92)81510-S

Grosjean H, de Crécy-Lagard V, Marck C. 2010. Deciphering synonymous codons in the three domains of life: co-evolution with specific tRNA modification enzymes. *FEBS Lett* **584:** 252–264. doi:10.1016/j.febslet.2009.11.052

Gu C, Ramos J, Begley U, Dedon PC, Fu D, Begley TJ. 2018. Phosphorylation of human TRM9L integrates multiple stress-signaling pathways for tumor growth suppression. *Sci Adv* **4:** eaas9184. doi:10.1126/sciadv.aas9184

Guerrier-Takada C, Gardiner K, Marsh T, Pace N, Altman S. 1983. The RNA moiety of ribonuclease P is the catalytic subunit of the enzyme. *Cell* **35:** 849–857. doi:10.1016/0092-8674(83)90117-4

Guy MP, Podyma BM, Preston MA, Shaheen HH, Krivos KL, Limbach PA, Hopper AK, Phizicky EM. 2012. Yeast Trm7 interacts with distinct proteins for critical modifications of the $tRNA^{Phe}$ anticodon loop. *RNA* **18:** 1921–1933. doi:10.1261/rna.035287.112

Guzzi N, Cieśla M, Ngoc PCT, Lang S, Arora S, Dimitriou M, Pimková K, Sommarin MNE, Munita R, Lubas M, et al. 2018. Pseudouridylation of tRNA-derived fragments steers translational control in stem cells. *Cell* **173:** 1204–1216. doi:10.1016/j.cell.2018.03.008

Hampel A, Enger MD. 1973. Subcellular distribution of aminoacyl-transfer RNA synthetases in Chinese hamster ovary cell culture. *J Mol Biol* **79:** 285–293. doi:10.1016/0022-2836(73)90006-5

Hedgcoth C, Hayenga K, Harrison M, Ortwerth BJ. 1984. Lysine tRNAs from rat liver: lysine tRNA sequences are highly conserved. *Nucleic Acids Res* **12:** 2535–2541. doi:10.1093/nar/12.5.2535

Heinz S, Benner C, Spann N, Bertolino E, Lin YC, Laslo P, Cheng JX, Murre C, Sing H, Glass CK. 2010. Simple combinations of lineage-determining transcription factors prime *cis*-regulatory elements required for macrophage and B cell identities. *Mol Cell* **38:** 576–589. doi:10.1016/j.molcel.2010.05.004

Holley CL, Li MW, Scruggs BS, Matkovich SJ, Ory DS, Schaffer JE. 2015. Cytosolic accumulation of small nucleolar RNAs (snoRNAs) is dynamically regulated by NADPH oxidase. *J Biol Chem* **290:** 11741–11748. doi:10.1074/jbc.M115.637413

Huang B. 2005. An early step in wobble uridine tRNA modification requires the Elongator complex. *RNA* **11:** 424–436. doi:10.1261/rna.7247705

Huang B, Lu J, Bystrom AS. 2008. A genome-wide screen identifies genes required for formation of the wobble nucleoside 5-methoxycarbonylmethyl-2-thiouridine in *Saccharomyces cerevisiae*. *RNA* **14:** 2183–2194. doi:10.1261/rna.1184108

Hussain S, Sajini AA, Blanco S, Dietmann S, Lombard P, Sugimoto Y, Paramor M, Gleeson JG, Odom DT, Ule J, et al. 2013. NSun2-mediated cytosine-5 methylation of vault noncoding RNA determines its processing into regulatory small RNAs. *Cell Rep* **4:** 255–261. doi:10.1016/j.celrep.2013.06.029

Inagaki Y, Kojima A, Bessho Y, Hori H, Ohama T, Osawa S. 1995. Translation of synonymous codons in family boxes by *Mycoplasma capricolum* tRNAs with unmodified uridine or adenosine at the first anticodon position. *J Mol Biol* **251:** 486–492. doi:10.1006/jmbi.1995.0450

Johansson MJO, Esberg A, Huang B, Bjork GR, Bystrom AS. 2008. Eukaryotic Wobble uridine modifications promote a functionally redundant decoding system. *Mol Cell Biol* **28:** 3301–3312. doi:10.1128/MCB.01542-07

Kalhor HR, Clarke S. 2003. Novel methyltransferase for modified uridine residues at the Wobble position of tRNA. *Mol Cell Biol* **23:** 9283–9292. doi:10.1128/MCB.23.24.9283-9292.2003

Keith G, Desgrès J, Pochart P, Heyman T, Kuo K C, Gehrke C W. 1990. Eukaryotic $tRNAs^{Pro}$: primary structure of the anticodon loop; presence of 5-carbamoylmethyluridine or inosine as the first nucleoside of the anticodon. *Biochim Biophys Acta* **1049:** 255–260. doi:10.1016/0167-4781(90)90095-J

Kim J-H, Lane WS, Reinberg D. 2002. Human Elongator facilitates RNA polymerase II transcription through chromatin. *Proc Natl Acad Sci* **99:** 1241–1246. doi:10.1073/pnas.251672198

Kishore S, Gruber AR, Jedlinski DJ, Syed AP, Jorjani H, Zavolan M. 2013. Insights into snoRNA biogenesis and processing from PAR-CLIP of snoRNA core proteins and small RNA sequencing. *Genome Biol* **14:** R45. doi:10.1186/gb-2013-14-5-r45

Kobayashi T, Irie T, Yoshida M, Takeishi K, Ukita T. 1974. The primary structure of yeast glutamic acid tRNA specific to the GAA codon. *Biochimica Biophys Acta* **366:** 168–181. doi:10.1016/0005-2787(74)90331-1

König J, Zarnack K, Rot G, Curk T, Kayikci M, Zupan B, Turner DJ, Luscombe NM, Ule J. 2010. iCLIP reveals the function of hnRNP particles in splicing at individual nucleotide resolution. *Nat Struct Mol Biol* **17:** 909–915. doi:10.1038/nsmb.1838

Kuntzel B, Weissenbach J, Wolff RE, Tumaitis-Kennedy TD, Lane BG, Dirheimer G. 1975. Presence of the methylester of 5-carboxymethyl uridine in the wobble position of the anticodon of $tRNA^{Arg}_{III}$ from brewer's yeast. *Biochimie* **57:** 61–70. doi:10.1016/S0300-9084(75)80110-6

Leary DJ, Terns MP, Huang S. 2004. Components of U3 snoRNA-containing complexes shuttle between nuclei and the cytoplasm and differentially localize in nucleoli: implications for assembly and function. *Mol Biol Cell* **15:** 281–293. doi:10.1091/mbc.e03-06-0363

Leidel S, Pedrioli PGA, Bucher T, Brost R, Costanzo M, Schmidt A, Aebersold R, Boone C, Hofmann K, Peter M. 2009. Ubiquitin-related modifier Urm1 acts as a sulphur carrier in thiolation of eukaryotic transfer RNA. *Nature* **458:** 228–232. doi:10.1038/nature07643

Leihne V, Kirpekar F, Vågbø CB, van den Born E, Krokan HE, Grini PE, Meza TJ, Falnes PØ. 2011. Roles of Trm9- and ALKBH8-like proteins in the formation of modified wobble uridines in *Arabidopsis* tRNA. *Nucleic Acids Res* **39:** 7688–7701. doi:10.1093/nar/gkr406

Lemus-Diaz N, Ferreira RR, Bohnsack KE, Gruber J, Bohnsack MT. 2020. The human box C/D snoRNA U3 is a miRNA source and miR-U3 regulates expression of sortin nexin 27. *Nucleic Acids Res* **48:** 8074–8089. doi:10.1093/nar/gkaa549

Lentini JM, Ramos J, Fu D. 2018. Monitoring the 5-methoxycarbonylmethyl-2-thiouridine (mcm5s2U) modification in eukaryotic tRNAs via the γ-toxin endonuclease. *RNA* **24:** 749–758. doi:10.1261/rna.065581.118

Li H, Handsaker B, Wysoker A, Fennell T, Ruan J, Homer N, Marth G, Abecasis G, Durbin R, 1000 Genome Project Data Processing Subgroup. 2009. The Sequence Alignment/Map format and SAMtools. *Bioinformatics* **25:** 2078–2079. doi:10.1093/bioinformatics/btp352

Li J, Wang Y-N, Xu B-S, Liu Y-P, Zhou M, Long T, Li H, Dong H, Nie Y, Chen PR, et al. 2020. Intellectual disability-associated gene ftsj1 is responsible for 2′-O-methylation of specific tRNAs. *EMBO Rep* **21:** e50095. doi:10.15252/embr.202050095

Lipowsky G, Bischoff FR, Izaurralde E, Kutay U, Schäfer S, Gross HJ, Beier H, Görlich D. 1999. Coordination of tRNA nuclear export with processing of tRNA. *RNA* **5:** 539–549. doi:10.1017/S1355838299982134

Lu J, Huang B, Esberg A, Johansson MJO, Byström AS. 2005. The *Kluyveromyces lactis* γ-toxin targets tRNA anticodons. *RNA* **11:** 1648–1654. doi:10.1261/rna.2172105

Maddirevula S, Alameer S, Ewida N, de Sousa MML, Bjørås M, Vågbø CB, Alkuraya FS. 2022. Insight into ALKBH8-related intellectual developmental disability based on the first pathogenic missense variant. *Hum Genet* **141:** 209–215. doi:10.1007/s00439-021-02391-z

Monies D, Vågbø CB, Al-Owain M, Alhomaidi S, Alkuraya FS. 2019. Recessive truncating mutations in ALKBH8 cause intellectual disability and severe impairment of Wobble uridine modification. *Am J Hum Genet* **104:** 1202–1209. doi:10.1016/j.ajhg.2019.03.026

Nakai Y, Nakai M, Hayashi H. 2008. Thio-modification of yeast cytosolic tRNA requires a ubiquitin-related system that resembles bacterial sulfur transfer systems. *J Biol Chem* **283:** 27469–27476. doi:10.1074/jbc.M804043200

Noma A, Sakaguchi Y, Suzuki T. 2009. Mechanistic characterization of the sulfur-relay system for eukaryotic 2-thiouridine biogenesis at tRNA wobble positions. *Nucleic Acids Res* **37:** 1335–1352. doi:10.1093/nar/gkn1023

Ohira T, Suzuki T. 2011. Retrograde nuclear import of tRNA precursors is required for modified base biogenesis in yeast. *Proc Natl Acad Sci* **108:** 10502–10507. doi:10.1073/pnas.1105645108

Ohshio I, Kawakami R, Tsukada Y, Nakajima K, Kitae K, Shimanoe T, Saigo Y, Hase H, Ueda Y, Jingushi K, et al. 2016. ALKBH8 promotes bladder cancer growth and progression through regulating the expression of survivin. *Biochem Biophys Res Commun* **477:** 413–418. doi:10.1016/j.bbrc.2016.06.084

Pastore C, Topalidou I, Forouhar F, Yan AC, Levy M, Hunt JF. 2012. Crystal structure and RNA binding properties of the RNA recognition motif (RRM) and AlkB domains in human AlkB homolog 8 (ABH8) an enzyme catalyzing tRNA hypermodification. *J Biol Chem* **287:** 2130–2143. doi:10.1074/jbc.M111.286187

Pintard L. 2002. Trm7p catalyses the formation of two 2′-*O*-methylriboses in yeast tRNA anticodon loop. *EMBO J* **21:** 1811–1820. doi:10.1093/emboj/21.7.1811

Pokholok DK, Hannett NM, Young RA. 2002. Exchange of RNA polymerase II initiation and elongation factors during gene expression *in vivo*. *Mol Cell* **9:** 799–809. doi:10.1016/S1097-2765(02)00502-6

Quinlan AR, Hall IM. 2010. BEDTools: a flexible suite of utilities for comparing genomic features. *Bioinformatics* **26:** 841–842. doi:10.1093/bioinformatics/btq033

R Core Team. 2020. *R: a language and environment for statistical computing*. R Foundation for Statistical Computing, Vienna, Austria.

Raba M, Limburg K, Burghagen M, Katze JR, Simsek M, Heckman JE, Rajbhandary UL, Gross HJ. 1979. Nucleotide sequence of three isoaccepting lysine tRNAs from rabbit liver and SV40-transformed mouse fibroblasts. *Eur J Biochem* **97:** 305–318. doi:10.1111/j.1432-1033.1979.tb13115.x

Ramírez F, Ryan DP, Grüning B, Bhardwaj V, Kilpert F, Richter AS, Heyne S, Dündar F, Manke T. 2016. deepTools2: a next generation web server for deep-sequencing data analysis. *Nucleic Acids Res* **44:** W160–W165. doi:10.1093/nar/gkw257

Randerath E, Gupta RC, Chia L-LSY, Randerath K. 1979. Yeast $tRNA^{Leu}_{UAG}$. Purification, properties and determination of the nucleotide sequence by radioactive derivative methods. *Eur J Biochem* **93:** 79–94. doi:10.1111/j.1432-1033.1979.tb12797.x

Rogalski M, Karcher D, Bock R. 2008. Superwobbling facilitates translation with reduced tRNA sets. *Nat Struct Mol Biol* **15:** 192–198. doi:10.1038/nsmb.1370

Rossmanith W, Tullo A, Potuschak T, Karwan R, Sbisà E. 1995. Human mitochondrial tRNA processing. *J Biol Chem* **270:** 12885–12891. doi:10.1074/jbc.270.21.12885

Saad AK, Marafi D, Mitani T, Du H, Rafat K, Fatih JM, Jhangiani SN, Coban-Akdemir Z, Baylor-Hopkins Center for Mendelian Genomics, Gibbs RA, et al. 2021. Neurodevelopmental disorder in an Egyptian family with a biallelic ALKBH8 variant. *Am J Med Genet A* **185:** 1288–1293. doi:10.1002/ajmg.a.62100

Safra M, Nir R, Farouq D, Vainberg Slutskin I, Schwartz S. 2017. TRUB1 is the predominant pseudouridine synthase acting on mammalian mRNA via a predictable and conserved code. *Genome Res* **27:** 393–406. doi:10.1101/gr.207613.116

Schaffrath R, Leidel SA. 2017. Wobble uridine modifications–a reason to live, a reason to die? *RNA Biol* **14:** 1209–1222. doi:10.1080/15476286.2017.1295204

Schiffer S, Rösch S, Marchfelder A. 2002. Assigning a function to a conserved group of proteins: the tRNA 3′-processing enzymes. *EMBO J* **21:** 2769–2777. doi:10.1093/emboj/21.11.2769

Selvadurai K, Wang P, Seimetz J, Huang RH. 2014. Archaeal Elp3 catalyzes tRNA wobble uridine modification at C5 via a radical mechanism. *Nat Chem Biol* **10:** 810–812. doi:10.1038/nchembio.1610

Shimada K, Nakamura M, Anai S, De Velasco M, Tanaka M, Tsujikawa K, Ouji Y, Konishi N. 2009. A novel human AlkB homologue, ALKBH8, contributes to human bladder cancer progression. *Cancer Res* **69:** 3157–3164. doi:10.1158/0008-5472.CAN-08-3530

Smith CJ, Teh HS, Ley AN, D'Obrenan P. 1973. The nucleotide sequences and coding properties of the major and minor lysine transfer ribonucleic acids from the haploid yeast *Saccharomyces cerevisiae* S288C. *J Biol Chem* **248:** 4475–4485. doi:10.1016/S0021-9258(19)43792-7

Songe-Moller L, van den Born E, Leihne V, Vagbo CB, Kristoffersen T, Krokan HE, Kirpekar F, Falnes PO, Klungland A. 2010. Mammalian ALKBH8 possesses tRNA methyltransferase activity required for the biogenesis of multiple wobble uridine modifications implicated in translational decoding. *Mol Cell Biol* **30:** 1814–1827. doi:10.1128/MCB.01602-09

Streit D, Shanmugam T, Garbelyanski A, Simm S, Schleiff E. 2020. The existence and localization of nuclear snoRNAs in *Arabidopsis thaliana* revisited. *Plants (Basel)* **9:** 1016. doi:10.3390/plants9081016

Szweykowska-Kulinska Z, Senger B, Keith G, Fasiolo F, Grosjean H. 1994. Intron-dependent formation of pseudouridines in the anticodon of *Saccharomyces cerevisiae* minor $tRNA^{Ile}$. *EMBO J* **13:** 4636–4644. doi:10.1002/j.1460-2075.1994.tb06786.x

Thüring K, Schmid K, Keller P, Helm M. 2016. Analysis of RNA modifications by liquid chromatography–tandem mass spectrometry. *Methods* **107:** 48–56. doi:10.1016/j.ymeth.2016.03.019

Tsujikawa K, Koike K, Kitae K, Shinkawa A, Arima H, Suzuki T, Tsuchiya M, Makino Y, Furukawa T, Konishi N, et al. 2007. Expression and sub-cellular localization of human ABH family molecules. *J Cell Mol Med* **11:** 1105–1116. doi:10.1111/j.1582-4934.2007.00094.x

Ule J, Jensen K, Mele A, Darnell RB. 2005. CLIP: a method for identifying protein–RNA interaction sites in living cells. *Methods* **37:** 376–386. doi:10.1016/j.ymeth.2005.07.018

Uren PJ, Bahrami-Samani E, Burns SC, Qiao M, Karginov FV, Hodges E, Hannon GJ, Sanford JR, Penalva LOF, Smith AD. 2012. Site identification in high-throughput RNA-protein interaction data. *Bioinformatics* **28:** 3013–3020. doi:10.1093/bioinformatics/bts569

Ustianenko D, Pasulka J, Feketova Z, Bednarik L, Zigackova D, Fortova A, Zavolan M, Vanacova S. 2016. TUT-DIS3L2 is a mammalian surveillance pathway for aberrant structured non-coding RNAs. *EMBO J* **35:** 2179–2191. doi:10.15252/embj.201694857

van den Born E, Vågbø CB, Songe-Møller L, Leihne V, Lien GF, Leszczynska G, Malkiewicz A, Krokan HE, Kirpekar F, Klungland A, et al. 2011. ALKBH8-mediated formation of a novel diastereomeric pair of wobble nucleosides in mammalian tRNA. *Nat Commun* **2:** 172. doi:10.1038/ncomms1173

Vitali P, Kiss T. 2019. Cooperative 2′-O-methylation of the wobble cytidine of human elongator $tRNA^{Met}$(CAT) by a nucleolar and a Cajal body-specific box C/D RNP. *Genes Dev* **33:** 741–746. doi:10.1101/gad.326363.119

Waqas A, Nayab A, Shaheen S, Abbas S, Latif M, Rafeeq MM, Al-Dhuayan IS, Alqosaibi AI, Alnamshan MM, Sain ZM, et al. 2022. Case report: biallelic variant in the tRNA methyltransferase domain of the AlkB homolog 8 causes syndromic intellectual disability. *Front Genet* **13:** 878274. doi:10.3389/fgene.2022.878274

Warda AS, Kretschmer J, Hackert P, Lenz C, Urlaub H, Höbartner C, Sloan KE, Bohnsack MT. 2017. Human METTL16 is a N^6-methyladenosine (m^6A) methyltransferase that targets pre-mRNAs and various non-coding RNAs. *EMBO Rep* **18:** 2004–2014. doi:10.15252/embr.201744940

Wei Y-F, Carter KC, Wang R-P, Shell BK. 1996. Molecular cloning and functional analysis of a human cDNA encoding an *Escherichia coli* AlkB homolog, a protein involved in DNA alkylation damage repair. *Nucleic Acids Res* **24:** 931–937. doi:10.1093/nar/24.5.931

Wolfe CL, Hopper AK, Martin NC. 1996. Mechanisms leading to and the consequences of altering the normal distribution of ATP(CTP): tRNA nucleotidyltransferase in yeast. *J Biol Chem* **271:** 4679–4686. doi:10.1074/jbc.271.9.4679

Yamamoto N, Yamaizumi Z, Yokoyama S, Miyazawa T, Nishimura S. 1985. Modified nucleoside, 5-carbamoylmethyluridine, located in the first position of the anticodon of yeast valine tRNA. *J Biochem* **97:** 361–364. doi:10.1093/oxfordjournals.jbchem.a135061

Yip MCJ, Keszei AFA, Feng Q, Chu V, McKenna MJ, Shao S. 2019. Mechanism for recycling tRNAs on stalled ribosomes. *Nat Struct Mol Biol* **26:** 343–349. doi:10.1038/s41594-019-0211-4

Yip MCJ, Savickas S, Gygi SP, Shao S. 2020. ELAC1 repairs tRNAs cleaved during ribosome-associated quality control. *Cell Rep* **30:** 2106–2114.e5. doi:10.1016/j.celrep.2020.01.082

Yokoyama S, Watanabe T, Murao K, Ishikura H, Yamaizumi Z, Nishimura S, Miyazawa T. 1985. Molecular mechanism of codon recognition by tRNA species with modified uridine in the first position of the anticodon. *Proc Natl Acad Sci* **82:** 4905–4909. doi:10.1073/pnas.82.15.4905

Yoshihisa T, Ohshima C, Yunoki-Esaki K, Endo T. 2007. Cytoplasmic splicing of tRNA in *Saccharomyces cerevisiae*. *Genes Cells* **12:** 285–297. doi:10.1111/j.1365-2443.2007.01056.x